Research Square

Preprints are preliminary reports that have not undergone peer review.
They should not be considered conclusive, used to inform clinical practice,
or referenced by the media as validated information.

Surface functionalization of polyamide 6.6 fabric with transfluthrin using an atmospheric- pressure hybrid corona–dielectric barrier discharge

Eduardo Sant'Ana Petraconi Prado
edu.petraconi@gmail.com
Instituto Tecnológico de Aeronáutica – ITA/DCTA
Marcelo José Duarte
Instituto Tecnológico de Aeronáutica – ITA/DCTA
Isabella Grinberg Francelino
Instituto Tecnológico de Aeronáutica – ITA/DCTA
Rodrigo Sávio Pessoa
Instituto Tecnológico de Aeronáutica – ITA/DCTA
Felipe de Souza Miranda
Instituto Tecnológico de Aeronáutica – ITA/DCTA
Gilberto Petraconi
Instituto Tecnológico de Aeronáutica – ITA/DCTA

Research Article

Keywords: Atmospheric-pressure plasma, corona–dielectric barrier discharge (C-DBD), plasma-assisted polymerization, polyamide 6.6 functionalization, insect-repellent textiles

Posted Date: June 30th, 2026

DOI: https://doi.org/10.21203/rs.3.rs-9891015/v1

License: This work is licensed under a Creative Commons Attribution 4.0 International License.
Read Full License

Additional Declarations: No competing interests reported.

Surface functionalization of polyamide 6.6 fabric with transfluthrin using an atmospheric-pressure hybrid corona–dielectric barrier discharge

Eduardo Sant'Ana Petraconi Prado [a*], Marcelo José Duarte [a, b], Isabella Grinberg Francelino [a], Rodrigo Sávio Pessoa [a], Felipe de Souza Miranda [a], Gilberto Petraconi [a]

[a] *Laboratório de Plasmas e Processos - LPP, Instituto Tecnológico de Aeronáutica – ITA/DCTA, São José dos Campos, SP, Brazil.*

[b] *Ipanema Indústria de Produtos Veterinários Ltda*

**e-mail: edu.petraconi@gmail.com*

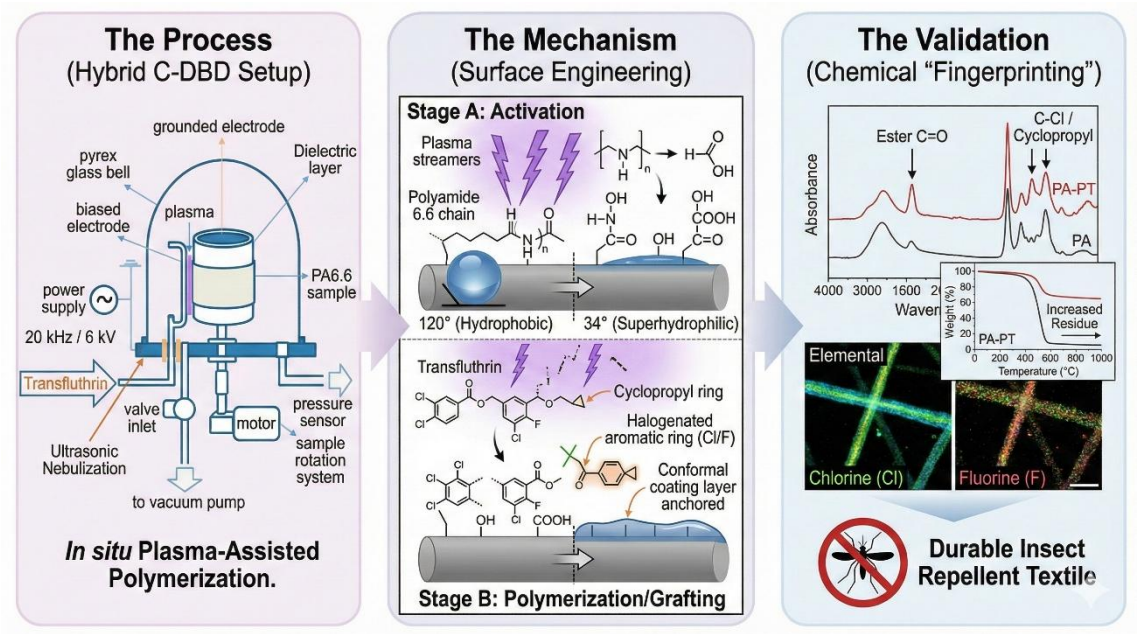
Abstract

This study investigates the surface functionalization of polyamide 6.6 fabric by plasma polymerization of transfluthrin (99%) using an atmospheric-pressure hybrid corona–dielectric barrier discharge (C-DBD). The process consists of an initial activation step of the polyamide fabric in a C-DBD operated in atmospheric air at 20 kHz and 6 kV, followed by exposure to liquid transfluthrin under the same discharge conditions to promote polymerization and fixation on the fiber surface. Electrical characterization indicated an average discharge power of 31.32 W and a plasma dosage of 1.3 $kW \cdot min \cdot m^{-2}$. Contact angle measurements showed a marked increase in wettability, favoring subsequent precursor spreading and reaction. Thermogravimetric analysis (TGA) revealed modifications in the thermal degradation profile of the functionalized samples. Fourier-transform infrared (FTIR) spectroscopy confirmed the formation of transfluthrin-derived polymeric structures on the fabric surface. Scanning Electron Microscopy (SEM) coupled with Energy-Dispersive Spectroscopy (EDS) confirmed the incorporation of transfluthrin-derived species along the fibers. Together, these results demonstrate that the process proposed enables the stable incorporation of transfluthrin on polyamide 6.6 fabrics, supporting its potential for advanced veterinary and healthcare

textile applications.

Keywords: Atmospheric-pressure plasma, corona–dielectric barrier discharge (C-DBD), plasma-assisted polymerization, polyamide 6.6 functionalization, insect-repellent textiles.

Graphical abstract



1. Introduction

In recent years, the development of functionalized fabrics has attracted growing attention because of their potential applications in healthcare, protective clothing, and advanced material engineering (Nadi et al. 2018; Muñoz et al. 2019; Hossain et al. 2025). Beyond their traditional role as passive substrates, fabrics can be engineered to exhibit antimicrobial activity, tunable hydrophobic or hydrophilic behavior, improved barrier properties, and insect-repellent functionalities (Luo and Van Ooij 2002; Kuhr et al. 2016; Bedrouni et al. 2024). A key challenge in this field is to modify the surface properties of polymeric fibers without compromising their bulk characteristics, mechanical integrity, and comfort for end users. Plasma-based surface modification techniques, particularly nonthermal plasmas operating at atmospheric pressure, have emerged as effective and environmentally friendly solutions to this challenge (Carneiro et al. 2006; Zhongfu et al. 2007; Morent et al. 2008; Javadzadeh and Hamedeyaz 2014; Singh et al. 2019). However, while plasma methods have been widely explored for the activation and functionalization of textiles, there are still relatively few studies on the plasma-assisted incorporation of pyrethroid insecticides such as transfluthrin on polyamide fabrics under atmospheric pressure, especially using hybrid corona–dielectric barrier discharge (C-DBD) systems. In addition, achieving durable, well-adhered insecticidal layers remains difficult because highly volatile active molecules tend to leach or desorb over time, reducing long-term repellency.

The hybrid corona–dielectric barrier discharge (C-DBD) system is a promising approach for atmospheric-pressure plasma processing of fabrics, as it combines the uniform, large-area treatment capability of dielectric barrier discharges with the localized high electric fields of corona discharges. This configuration enables efficient activation of polymer surfaces and the deposition or polymerization of thin functional coatings (Tsafack and

Levalois-Grützmacher 2006; Gawish et al. 2007; Morro et al. 2017; Peran and Ercegović Ražić 2020; Mou et al. 2024). By introducing polar functional groups (–OH, –COOH, –C=O, $–NH_2$), increasing surface roughness, and enhancing surface energy, C-DBD treatment improves wettability and adhesion (Vu et al. 2013; Ribeiro et al. 2020; Petraconi et al. 2023; Mou et al. 2024; Grinberg Francelino et al. 2025; SHEN 沈 et al. 2025; Francelino et al. 2025), which are key prerequisites for firmly anchoring insecticidal or repellent molecules to textile fibers. Furthermore, the DBD configuration allows direct nebulization of liquid or gaseous precursors into the plasma zone, enabling the formation of uniform, nanostructured, and potentially durable films under mild, near-ambient conditions (Abd El-Latif et al. 2024; SHEN 沈 et al. 2025; Fatahian and Erfani 2025). In the context of insect- and parasite-repellent textiles, these attributes are particularly attractive because they can promote both the controlled spreading of the precursor and its subsequent plasma-assisted grafting or polymerization on the fiber surface.

The versatility of DBD-based processes for textile functionalization has been demonstrated in several recent studies. Ribeiro et al. (Ribeiro et al. 2018) and Zille et al. (Zille et al. 2015) reported the deposition of silver nanoparticles on polyamide fabrics and investigated how aging affects the antimicrobial performance of samples treated with atmospheric DBD plasma. Francelino et al. (Francelino et al. 2025) achieved uniform incorporation of silver nanoparticles (AgNPs) on polyamide 6.6 fabrics, obtaining significant antimicrobial activity without inducing cytotoxicity. In another study, Francelino et al. (Grinberg Francelino et al. 2025) successfully deposited silica thin films on polyamide using silicic acid precursors, leading to controlled changes in wettability and the formation of nanostructured coatings. Similarly, Petraconi et al. (Petraconi et al. 2023) investigated the plasma polymerization of permethrin, a synthetic pyrethroid insecticide, and demonstrated that plasma-assisted processes can immobilize repellents

on fabric fibers more effectively than conventional impregnation methods, providing more homogeneous and durable coatings. These works highlight that atmospheric-pressure DBD and hybrid C-DBD systems can be tailored to activate textile substrates and to promote in situ polymerization or fixation of functional organic species.

Building on these advances, there is a growing interest in extending plasma-assisted approaches to other pyrethroids with higher volatility and insecticidal potency, such as transfluthrin. Transfluthrin is a fast-acting, highly volatile pyrethroid widely used in household and vector-control applications (Sukkanon et al.; Wagman et al. 2015; Achee and Grieco 2018). It acts on the insect nervous system by disrupting sodium channel function, causing paralysis and death. Compared with permethrin and icaridin (picaridin), transfluthrin exhibits enhanced vapor-phase repellency, making it particularly suitable for mosquito nets, tents, uniforms, and other protective fabrics (Vesin et al. 2013; Wagman et al. 2015). However, conventional functionalization methods, such as dipping, spraying, or polymer coating, often suffer from poor durability, limited adhesion, and rapid leaching of the active compound, which significantly reduces long-term effectiveness (Ojstršek et al. 2022; Tawiah et al. 2025; Ghosh et al. 2025). In this context, plasma polymerization or plasma-assisted grafting of transfluthrin onto polyamide fibers represents a promising strategy to improve the stability and retention of the active species while maintaining the mechanical and comfort properties of the fabric.

Therefore, the present work aims (i) to optimize the operation of a hybrid corona–dielectric barrier discharge at atmospheric pressure for the surface activation of polyamide 6.6 fabric and (ii) to investigate the plasma-assisted polymerization and fixation of transfluthrin on the fabric surface. To this end, electrical diagnostics of the C-DBD process are combined with wettability measurements, thermogravimetric analysis (TGA), Fourier-transform infrared (FTIR) spectroscopy, and Scanning Electron Microscopy (SEM) coupled with Energy-Dispersive Spectroscopy (EDS), in order to

correlate discharge characteristics with the physicochemical modifications induced on the textile and to assess the potential of this approach for developing insect- and parasite-repellent functional fabrics.

2. Materials and methods

2.1. Polyamide substrates, sample nomenclature and transfluthrin precursor

The polyamide substrate consisted of a half-knitted fabric composed of 92 wt% polyamide 6.6 and 8 wt% elastane (Rhodia Solvay), manufactured on fine-gauge machinery (38 needles per inch) with an areal density of 180 g m^{-2}. Specimens were cut into 25 × 60 cm pieces. Prior to plasma processing, the fabric underwent a standard "Ready-to-Dye" (RTD) pre-treatment to remove residual finishing agents and improve the reproducibility of subsequent wetting and uptake. The RTD step was performed by washing the specimens in an aqueous bath containing detergent (1.0 g L^{-1}) and sodium carbonate (1.0 g L^{-1}) at 60 °C for 20 min, following the baseline procedure previously adopted in our hybrid corona–DBD textile studies [17,34].

For consistency, the samples are identified using the codes listed in Table 1.

Table 1. Sample codes and corresponding descriptions used throughout the study for untreated, plasma-activated, and transfluthrin-treated polyamide 6.6 fabrics.

Code	Description
PA	Untreated (non-activated) polyamide 6.6 fabric
PA-P	Polyamide 6.6 after C-DBD plasma activation
PA-T	Polyamide 6.6 with transfluthrin, without plasma treatment
PA-PT	Polyamide 6.6 with transfluthrin and C-DBD plasma treatment

Transfluthrin was supplied by IPANEMA (Industry of Veterinary Products, Brazil) and had been originally purchased from Bayer Vapi Private Limited (India). Transfluthrin is

a highly volatile pyrethroid insecticide, chemically defined as 2,3,5,6-tetrafluorobenzyl (1RS,3RS;1RS,3SR)-3-(2,2-dichlorovinyl)-2,2-dimethylcyclopropane-1-carboxylate ($C_{15}H_{12}Cl_2F_4O_2$). According to the certificate of analysis, the batch used in this study had a purity of 99.0%, with a reported H_2SO_3 content of 0.009% and a moisture content of 0.016%. The precursor was used as received, without additional purification, and its introduction into the plasma zone is described in Section 2.2.

2.2. Plasma reactor, processing conditions and treatment protocol

Plasma processing was performed using a hybrid corona–dielectric barrier discharge (C-DBD) system (Figure 1). The setup comprises a high-voltage electrode facing a grounded electrode covered by a silicone-based dielectric barrier (5 mm thick), with the textile positioned at a 2 mm gap from the dielectric. This spacing was selected based on preliminary trials to ensure a stable discharge that spans the full interelectrode region, thereby promoting uniform exposure across the effective treatment width. The power supply delivers AC excitation with tunable frequency (10–30 kHz) and peak voltage up to 15 kV; in this study, all experiments were conducted in ambient air (atmospheric pressure, room humidity) at 20 kHz, 6 kV voltage amplitude, and an average discharge power of 31.32 W, using the same electrical settings for both activation (PA → PA-P) and plasma-assisted polymerization (PA-T → PA-PT). Although the platform is compatible with reduced-pressure operation, the results reported here correspond exclusively to atmospheric processing conditions.

For precursor delivery, an ultrasonic nebulization unit was coupled to the reactor to generate an aerosol from liquid transfluthrin and introduce it directly into the discharge zone through a channel integrated into the high-voltage electrode. This configuration enables interaction of aerosol droplets and vapor-phase fragments with the active plasma region immediately upstream of the textile surface, favoring in situ formation and

immobilization of transfluthrin-derived species. The fabric samples were fixed on a rotating transport stage; exposure was controlled by the number of passes through the discharge region and by the linear velocity of the stage. In the present work, the number of passes was maintained at P = 4, with substrate velocity V = 7.4 × 10^{-2} m·min^{-1} and effective treatment width L = 0.13 m. After processing, specimens were sealed under vacuum in plastic bags to reduce uncontrolled contamination and post-treatment aging prior to characterization.

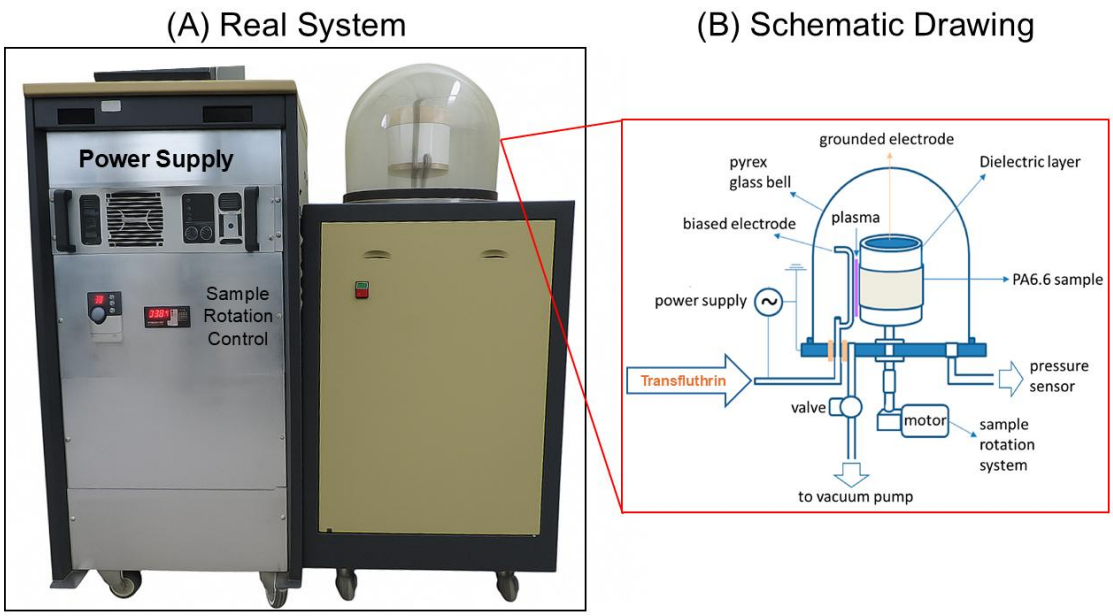


Figure 1. Experimental setup used for plasma activation and plasma-assisted polymerization of polyamide fabrics. (A) Photograph of the real hybrid corona–dielectric barrier discharge (C-DBD) system. (B) Schematic representation of the C-DBD reactor.

2.3. Electrical characterization of the discharge

Electrical characterization of the C-DBD was carried out using a digital oscilloscope (DSOX1202A, Keysight Technologies) together with a high-voltage probe (P6015A, Tektronix Inc.) and a passive probe (N2863B, Agilent Technologies). Voltage and current waveforms were recorded simultaneously over several AC periods, and the average discharge power was obtained by time-averaging the instantaneous $V(t)I(t)$product over

one excitation period; the plasma dosage was then computed from the measured discharge power and the transport parameters (passages, velocity, and effective treatment width).

2.4. Characterization techniques

Water contact angles were measured by the sessile-drop method using a dynamic contact-angle analyzer (FTA 1000, First Ten Ångstroms) with goniometric profile analysis. For each measurement, a 6 µL droplet of deionized water was deposited on the fabric surface. To account for the inherent heterogeneity of the textile, readings were collected at multiple locations on each specimen, and the reported values correspond to the average of these measurements.

Thermogravimetric analysis was carried out using a simultaneous thermal analyzer (STA 449 F3, Netzsch) with approximately 9 mg of sample. Measurements were performed under synthetic air while heating from 30 to 600 °C at 10 °C min^{-1}, and both the mass-loss (TG) curves and their derivatives (DTG) were analyzed to identify changes associated with plasma activation and the formation of transfluthrin-derived surface material.

FTIR-ATR spectra were acquired with a spectrometer (Spotlight 400, PerkinElmer). For each sample, spectra were collected as the average of 64 scans over the 400–3500 cm^{-1} range with 4 cm^{-1} resolution, and the bands were examined to identify contributions from the polyamide backbone and features attributable to transfluthrin-derived species and plasma-induced functionalization.

Surface morphology was examined by scanning electron microscopy using a SEM (Mira 3, Tescan) equipped with an EDS detector. SEM micrographs were obtained for PA, PA-P, and PA-PT to evaluate plasma-induced morphological changes and to assess the presence of surface-associated deposited material after transfluthrin-assisted treatment. EDS spectra and elemental maps were collected to detect and spatially map transfluthrin-

characteristic elements, with particular attention to chlorine and fluorine on the fiber network.

3. Results and discussion

3.1. Electrical discharge characterization

The electrical behavior of the hybrid corona–dielectric barrier discharge (C-DBD) was first characterized to establish the operating regime and quantify the energy delivered to the samples. Plasma excitation was achieved using a duty-cycle sinusoidal voltage with a peak amplitude of 6 kV at a frequency of 20 kHz, as shown in Figure 2. This excitation mode is typical of atmospheric-pressure DBD systems, where the alternating high voltage promotes repetitive breakdown events while the dielectric barrier suppresses the transition to an arc regime.

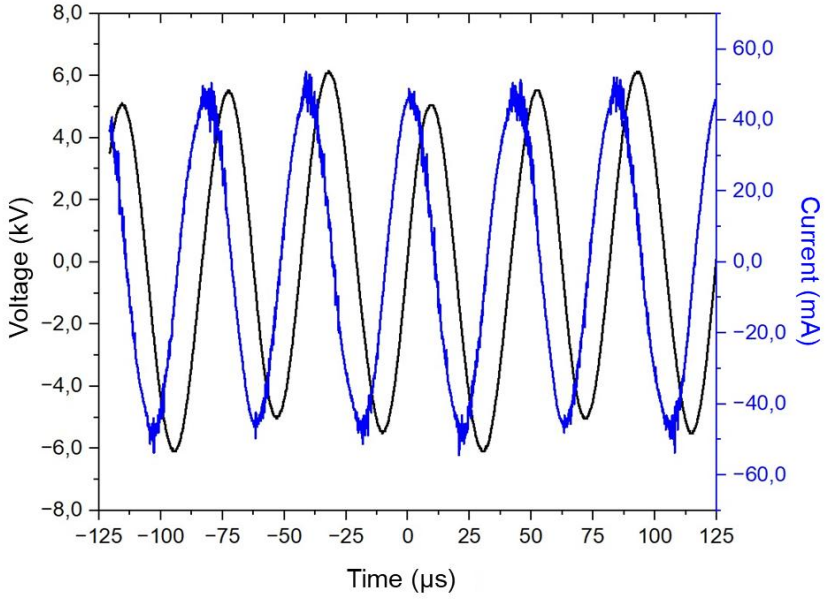


Figure 2. Time-resolved voltage and current waveforms of the hybrid corona–dielectric barrier discharge (C-DBD) operated in atmospheric air.

The measured current waveform (Figure 2A) consists of a capacitive background current superimposed with numerous sharp current spikes. These spikes correspond to transient

microdischarges occurring randomly in time and space during each half-cycle of the applied voltage. Such a discharge structure is characteristic of non-thermal DBD and hybrid C-DBD plasmas and ensures that the energy is distributed over multiple localized events rather than concentrated in a single filament, thereby preserving low gas temperature and minimizing thermal damage to polymeric substrates (Nascimento et al. 2020). Under the selected operating conditions, the average discharge power was 31.32 W, calculated from the time integration of the instantaneous voltage–current product. This moderate power level, combined with atmospheric-pressure operation, is particularly suitable for textile processing, as it enables efficient surface activation while maintaining the structural integrity of the fibers.

3.2. Wettability evolution and plasma activation of polyamide

The effect of plasma activation on the surface properties of the polyamide fabric was first evaluated through water contact angle (WCA) measurements, which provide a sensitive probe of surface chemistry and energy. Figure 3 summarizes the wettability evolution of PA and PA-P samples as a function of time after plasma exposure, for a plasma dosage of 1.3 $kW \cdot min \cdot m^{-2}$.

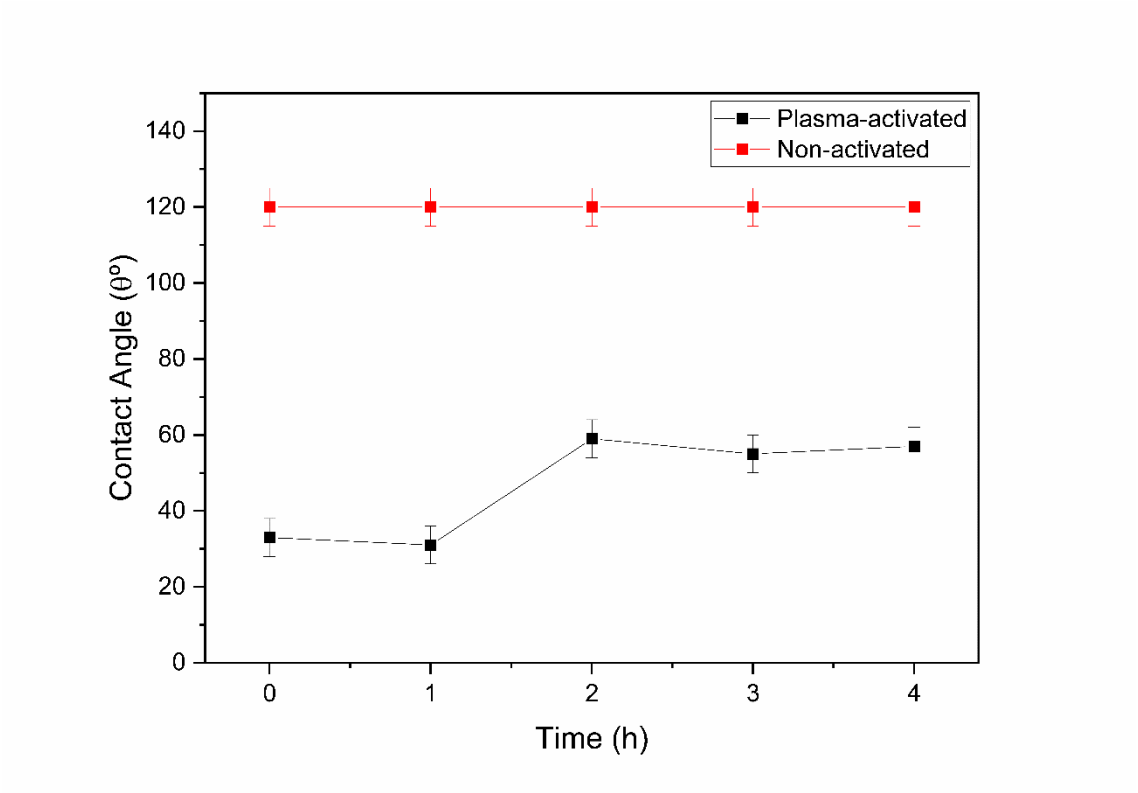


Figure 3. Temporal evolution of the water contact angle of polyamide 6.6 fabrics as a function of aging time after plasma treatment at a dosage of 1.3 kW·min·m^{-2}.

The untreated PA exhibited a strongly hydrophobic surface, with a static contact angle of approximately 120°. After plasma activation (PA-P), the contact angle decreased sharply to 34°, indicating a pronounced increase in surface hydrophilicity. Immediately after treatment, the surface displayed superhydrophilic behavior, with complete spreading of the water droplet (contact angle ≈ 0°). This behavior is attributed to the incorporation of polar oxygen- and nitrogen-containing functional groups (–OH, –COOH, –C=O, –NH) induced by reactive plasma species generated in air, combined with mild surface etching that increases effective roughness and surface energy (Bedrouni et al. 2024).

Aging effects were also observed. Within the first hour after treatment, the contact angle stabilized at approximately 34°, followed by a partial hydrophobic recovery over 2–4 h, reaching values close to 60°. This recovery is commonly reported for plasma-treated polymers and is associated with reorientation of polar groups toward the bulk and adsorption of airborne contaminants [6]. Despite this partial recovery, the activated

samples remained significantly more hydrophilic than the untreated fabric, indicating that a substantial fraction of the plasma-induced surface modification was retained. These wettability changes provide indirect evidence of chemical activation of the outermost surface, which is a prerequisite for subsequent plasma-assisted polymerization of transfluthrin.

3.3. FTIR analysis of plasma-activated polyamide

To correlate the wettability changes with chemical modifications, FTIR-ATR spectroscopy was performed on PA and PA-P samples (Figure 4). As expected, the overall spectra of the untreated and plasma-activated fabrics are largely similar, reflecting the fact that FTIR-ATR probes a depth of several micrometers, whereas plasma modification is confined primarily to the outermost nanometric surface layer.

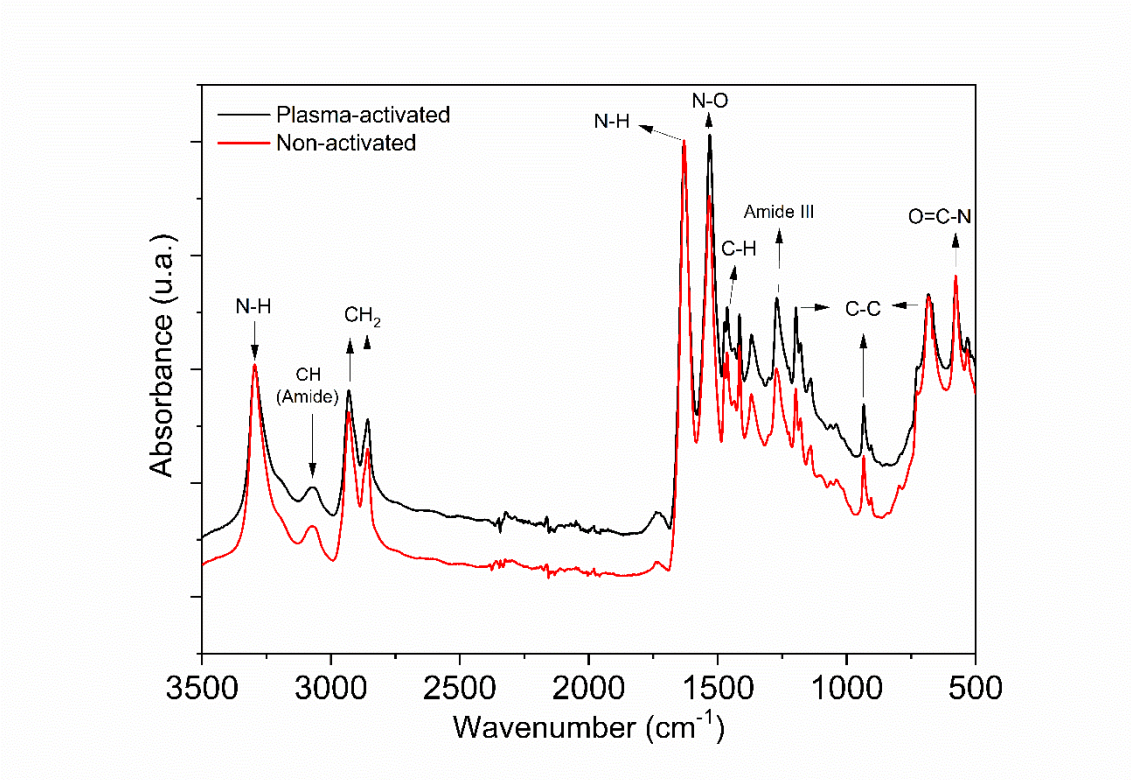


Figure 4. FTIR-ATR spectra of non-activated (PA, red curve) and plasma-activated (PA-P, black curve) polyamide 6.6 fabrics.

Nevertheless, subtle changes in absorbance intensity can be discerned. Variations were observed in bands associated with C–H stretching and in regions related to N–O and

oxygen-containing functionalities, suggesting an increased concentration of polar groups after plasma treatment (Petraconi et al. 2023; Singh et al. 2023). The positions of the characteristic amide I, II, and III bands remained unchanged, indicating that the polyamide backbone was not chemically degraded under the relatively mild C-DBD conditions employed. This behavior is consistent with previous reports on atmospheric-pressure plasma treatment of polyamide 6.6, where surface activation occurs without the formation of new bulk chemical groups detectable by FTIR (Petraconi et al. 2023; Singh et al. 2023; Grinberg Francelino et al. 2025). The limited spectral changes therefore corroborate a shallow, surface-confined modification, in agreement with the electrical characteristics of the discharge and the observed wettability enhancement.

3.4 Transfluthrin polymerization: thermal and spectroscopic evidence

3.4.1. Thermogravimetric analysis

Thermogravimetric analysis was used to assess the effect of plasma-assisted transfluthrin polymerization on the thermal behavior of the fabric. Figure 5 compares the TGA curves of the untreated polyamide (PA) and the transfluthrin-polymerized sample (PA-PT) obtained after four plasma passages.

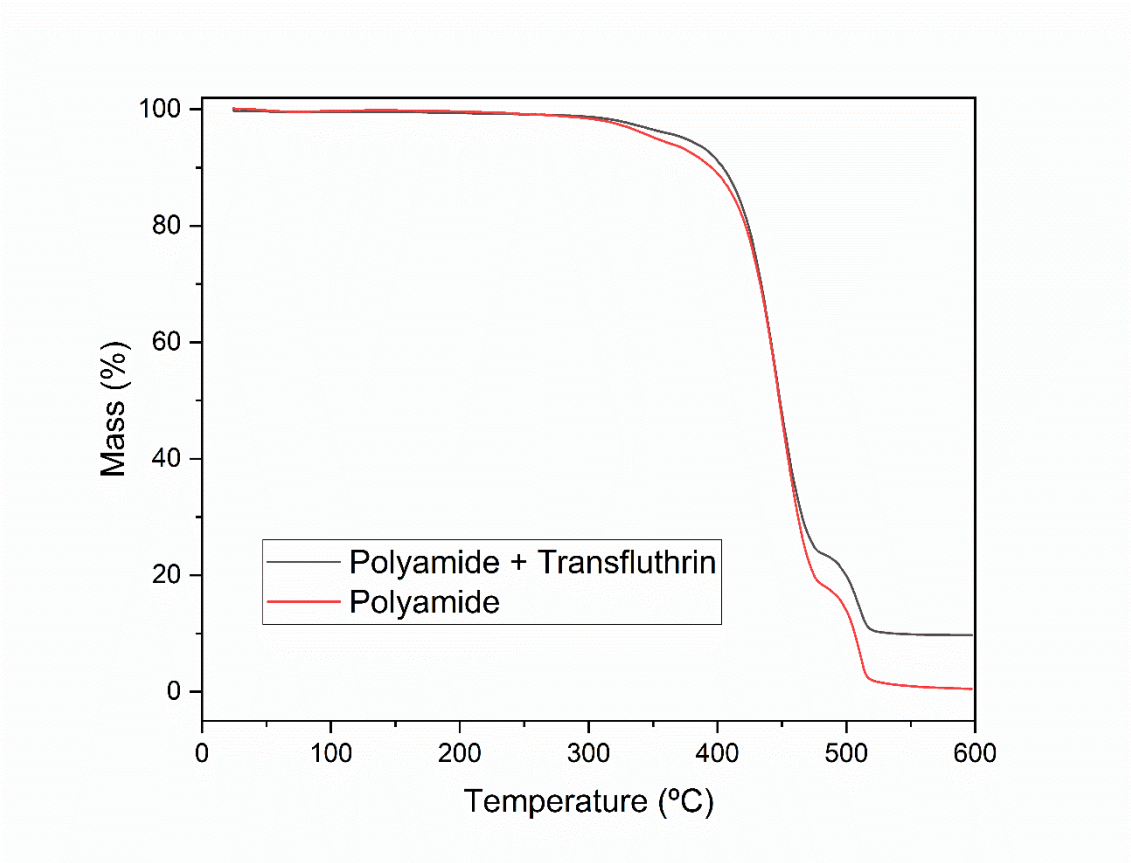


Figure 5. Thermogravimetric analysis (TGA) curves of untreated polyamide 6.6 fabric (PA, red curve) and transfluthrin-polymerized polyamide fabric (PA-PT, black curve) after four plasma polymerization passages.

Both samples exhibit a similar overall mass-loss profile, with negligible weight loss below approximately 350 °C, followed by a major degradation step between 350 and 450 °C, corresponding to thermal decomposition of the polyamide backbone. However, the PA-PT sample shows a higher residual mass at the end of the analysis, which is not present in the untreated fabric. This additional residue is attributed to the presence of transfluthrin-derived polymeric material deposited or grafted onto the fiber surface. The absence of a distinct low-temperature mass-loss step suggests that the transfluthrin is not merely physically adsorbed but is stabilized on the surface, consistent with plasma-induced polymerization or strong interfacial bonding.

3.4.2. FTIR evidence of transfluthrin incorporation

Figure 6 compares the FTIR-ATR spectra of the transfluthrin precursor, the non-activated polyamide fabric (PA), and the plasma-polymerized fabric (PA-PT). This comparative

analysis allows the identification of spectral features associated with transfluthrin-derived structures and their evolution upon plasma-assisted polymerization on the polyamide surface.

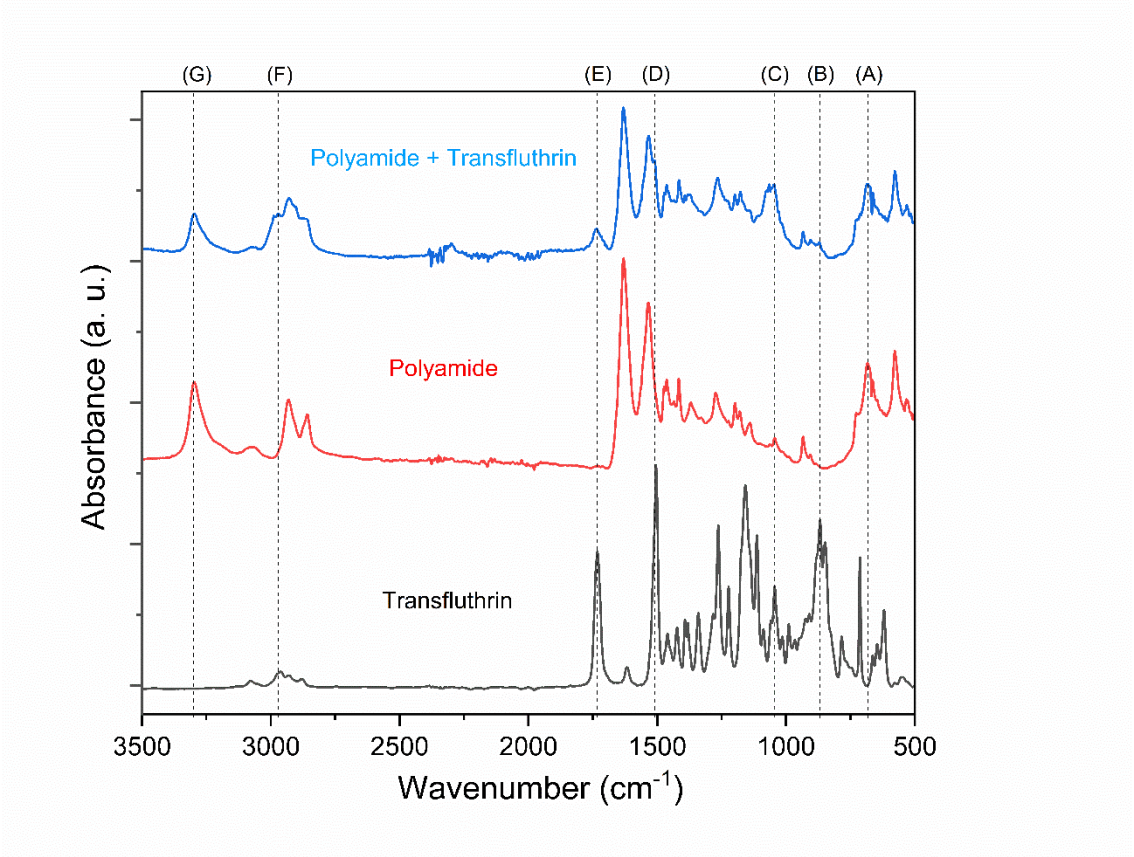


Figure 6. FTIR-ATR spectra of the transfluthrin precursor (black curve), non-activated polyamide 6.6 fabric (PA, red curve), and plasma-polymerized polyamide fabric (PA-PT, blue curve).

In the low-wavenumber region, the band at approximately 648 cm^{-1}, attributed to asymmetric C–Cl stretching vibrations characteristic of transfluthrin, overlaps with a band present in the polyamide spectrum associated with out-of-plane N–H or O–H deformations [39]. As indicated by the dashed guides in Figure 6, such overlap complicates direct assignment; however, changes in band intensity and shape in the PA-PT spectrum suggest the contribution of chlorine-containing species originating from transfluthrin.

The band located near 690 cm^{-1} (region A), assigned to out-of-plane vibrations of the substituted benzene ring in transfluthrin [40], is not clearly resolved in the polymerized

sample. This attenuation is likely due to overlap with the polyamide band around 700 cm^{-1}, commonly associated with N–H link defects [39], as well as to plasma-induced fragmentation and recombination processes that modify the aromatic environment. In contrast, a discernible spectral change appears around 880 cm^{-1} (region B), associated with C–C vibrations and benzene ring deformation modes [39]. These features are absent in the untreated polyamide but become evident after plasma-assisted polymerization, indicating incorporation of transfluthrin-derived fragments.

The most pronounced modification in the PA-PT spectrum occurs at approximately 1045 cm^{-1} (region C), which is assigned to vibrational modes of the cyclopropyl group. The emergence and enhancement of this band are indicative of strong interactions between cyclopropyl-containing fragments of transfluthrin and the plasma-activated polyamide surface, supporting the occurrence of plasma-induced grafting or polymerization.

In the mid-infrared region, the band at 1505 cm^{-1} (region D) corresponds to C=C stretching vibrations of the substituted aromatic ring, which is a defining structural element of pyrethroid compounds and contributes to their chemical stability and lipophilicity [41,42]. Additionally, the absorption band at 1734 cm^{-1} (region E) is attributed to C=O stretching of the ester functional group, a hallmark of pyrethroids typically observed between 1730 and 1750 cm^{-1} [38,41–43]. The persistence of these bands in the PA-PT spectrum confirms that key structural motifs of transfluthrin—namely the halogenated aromatic ring and the ester group—are retained after plasma processing, despite partial fragmentation.

Alterations are also observed in the high-wavenumber region. The band around 2965 cm^{-1} (region F), associated with asymmetric CH_3 stretching vibrations, shows noticeable modification in the polymerized sample. This behavior is attributed to the superposition of polyamide and transfluthrin contributions and reflects plasma-induced chemical restructuring at the surface. Furthermore, the broad band centered near 3300 cm^{-1} (region

G) is assigned to N–H stretching vibrations, commonly referred to as Amide Band A in polyamides [44]. Its width and intensity are influenced by hydrogen bonding and surface polarity, both of which are affected by plasma activation and subsequent polymerization. Additional vibrational features remain identifiable across the spectra, including C–H stretching modes of aromatic rings at 3064 and 3044 cm^{-1}, benzene ring C=C stretching at 1587, 1489, and 1447 cm^{-1}, and symmetric and asymmetric CH_2/CH_3 stretching modes at 2963, 2925, and 2876 cm^{-1} [17,38]. Deformation modes of CH_2 groups (1379 cm^{-1}), cyclopropyl group vibrations (1418 and 1338 cm^{-1}), and ester-related C–O–C stretching at 1256 cm^{-1} are also observed [39,45–48]. Characteristic amide bands of the polyamide backbone (Amide I, II, and III) remain present, confirming that the polymer matrix is preserved during plasma treatment [18,19,51].

Taken together, the FTIR results provide strong spectroscopic evidence that transfluthrin is not merely physically adsorbed but is chemically incorporated in the near-surface region of the polyamide fabric through plasma-assisted polymerization. The coexistence of transfluthrin-specific bands with preserved polyamide features, combined with their modification in intensity and shape, supports a mechanism involving plasma-induced fragmentation of the precursor followed by recombination and stabilization on the activated polymer surface.

3.5. Surface morphology and elemental composition

The morphological and compositional analyses were used to verify whether the hybrid C-DBD protocol induces only mild topographical changes on polyamide 6.6 fibers while enabling the incorporation of transfluthrin-derived species. As established in the wettability results (Section 3.2), air plasmas increase the surface energy of polyamide mainly through the introduction of polar oxygen- and nitrogen-containing functionalities and through limited etching/ablation of the outermost layer, which together promote

precursor spreading and interfacial adhesion [8,14,34,37]. In this context, the activated surface provides both chemically reactive sites and a higher density of adsorption/anchoring points that favor subsequent plasma-assisted fragmentation–recombination pathways, leading to the formation of an immobilized, transfluthrin-derived layer rather than a purely physisorbed deposit [17,37]. This coupling between activation and deposition is schematically summarized by the chemical structures shown in Figure 7, which highlights the amide-rich backbone of polyamide and the halogenated/ester functionalities of transfluthrin that serve as diagnostic markers for incorporation (Figure 7).

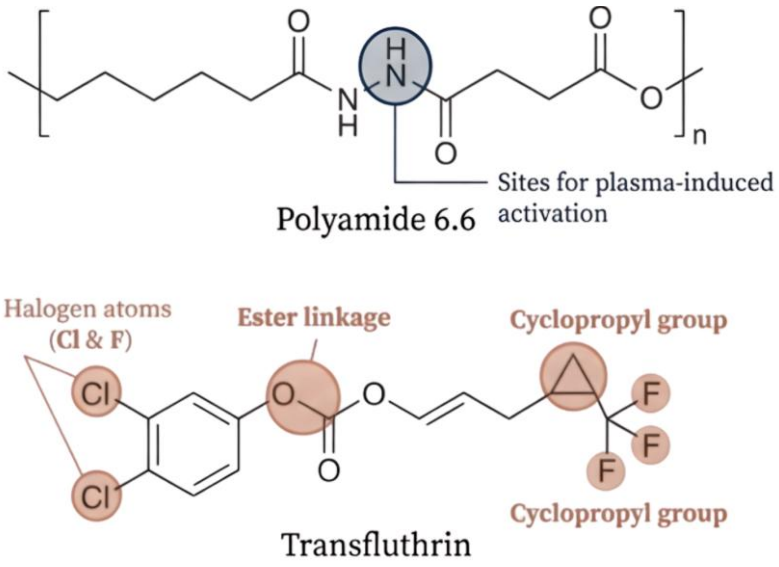


Figure 7. Schematic chemical structures of polyamide 6.6 and transfluthrin.

SEM observations (Figure 8) indicate that the selected operating window produces only minor morphological changes, consistent with non-thermal textile processing. The untreated fibers (PA; Figure 8A) show the expected smooth surface. After plasma activation (PA-P; Figure 8B), the fiber surface exhibits a discernible increase in apparent roughness, which is consistent with shallow etching and localized restructuring reported for atmospheric DBD/C-DBD treatments of polyamide and related polymers [8,34,37]. Importantly, after plasma-assisted polymerization (PA-PT; Figure 8C), the fibers appear more homogeneous and partially “smoothed” relative to PA-P. This behavior is consistent

with the formation of a thin, conformal transfluthrin-derived coating that covers or fills the nanoscale features generated during activation, while still preserving the macroscopic integrity of the fibers (i.e., no evidence of melting, severe cracking, or fiber collapse at the applied conditions). The SEM trends therefore support a sequence in which activation creates a higher-energy, more receptive surface, followed by deposition/grafting that yields a more uniform outer layer, in agreement with the thermal and FTIR indications of stabilized transfluthrin-derived material (Sections 3.4.1–3.4.2) [17,37].

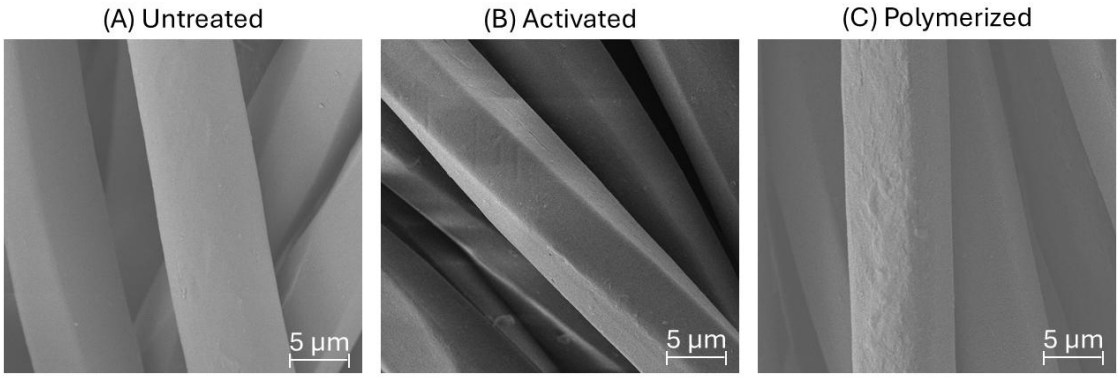


Figure 8. SEM micrographs of polyamide 6.6 fibers: (A) untreated fabric (PA); (B) plasma-activated fabric (PA-P), showing a more textured surface consistent with mild surface modification; (C) fabric after plasma processing with transfluthrin (PA-PT).

Elemental analysis by EDS provides a complementary and more direct signature of transfluthrin incorporation because chlorine and fluorine are not constituents of the pristine polyamide 6.6 substrate and can thus be used as chemical fingerprints of pyrethroid-derived species on the fibers. In the elemental maps acquired from PA-PT (Figure 9), signals from C and O are expected from the polymer backbone and any oxygenated functionalities formed during plasma exposure, whereas the detection of Cl and F indicates the presence of halogenated fragments associated with transfluthrin (Figure 9). The broadly distributed Cl and F signals across the mapped fiber network suggest that incorporation is not restricted to isolated spots (e.g., droplet residues), but occurs over the treated surface in a comparatively homogeneous manner, consistent with aerosol/vapor interaction in the active plasma zone and with the uniform treatment

strategy used here [17,34,37]. While EDS does not resolve chemical bonding states and is inherently semi-quantitative—particularly for thin surface layers on polymeric substrates—its agreement with FTIR band evolution and with the increased thermal residue in TGA strengthens the interpretation that the process results in a stabilized, transfluthrin-derived layer rather than transient adsorption [17,37]. Taken together, Figures 7–9 support the mechanistic picture that C-DBD activation primes the polyamide surface for adhesion, and subsequent plasma exposure in the presence of transfluthrin promotes fragmentation and recombination routes that immobilize halogen-containing species on the fibers with minimal morphological degradation of the textile.

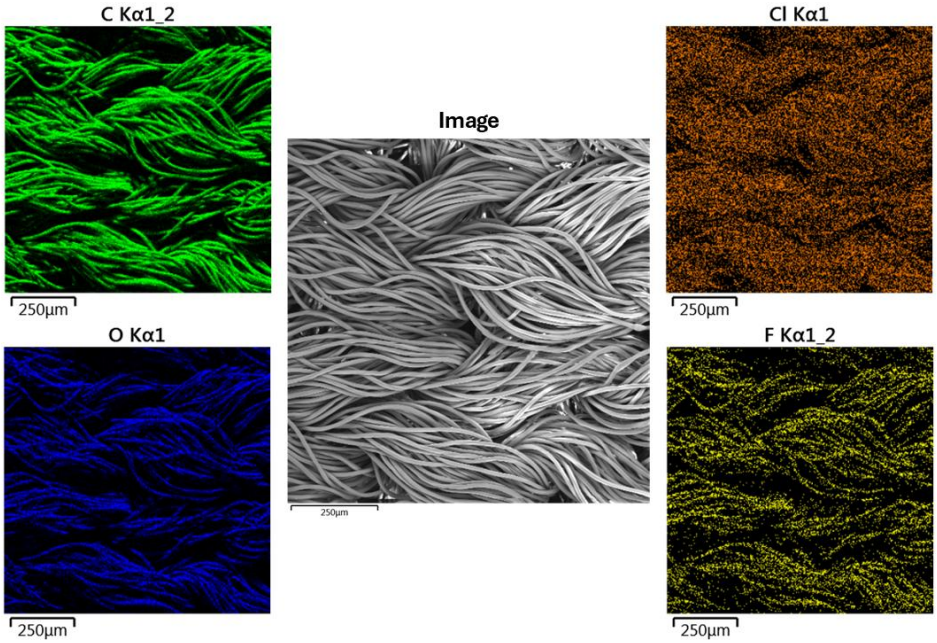


Figure 9. SEM micrograph and EDS elemental maps of the polyamide 6.6 fabric after plasma processing with transfluthrin (PA-PT).

4 Conclusion

This study demonstrated the surface functionalization of polyamide 6.6 fabrics by plasma activation and in situ plasma-assisted polymerization of transfluthrin using an atmospheric-pressure hybrid corona–dielectric barrier discharge (C-DBD). The discharge

operated in a stable non-thermal regime under sinusoidal excitation (6 kV, 20 kHz), delivering an average power of 31.32 W and enabling uniform treatment without compromising fiber integrity. Plasma activation significantly enhanced surface wettability, reducing the water contact angle from approximately 120° to 34°, due to the incorporation of polar functional groups and mild surface etching. Subsequent plasma-assisted polymerization led to the stable incorporation of transfluthrin on the fiber surface. This was confirmed by thermogravimetric analysis, FTIR spectroscopy, and SEM–EDS, which revealed transfluthrin-derived chemical structures, increased thermal residue, and homogeneous distributions of chlorine and fluorine along the fibers. Overall, the results show that hybrid C-DBD processing enables controlled and durable functionalization of polyamide fabrics with highly volatile pyrethroid compounds under mild, atmospheric-pressure conditions, offering a promising route for the development of insect- and parasite-repellent textiles for veterinary and healthcare applications.

Acknowledgments

The authors also acknowledge IPANEMA – Industry of Veterinary Products and the Plasmas and Processes Laboratory (LPP) at the Aeronautics Institute of Technology (ITA) for their technical and institutional support.

Funding Statement: The study was supported by assistant researcher grant from the IPANEMA - Industry of Veterinary Products. This work was carried out under research program post-doctoral of the Technological Institute of Aeronautics. Author Eduardo Sant'Ana Petraconi Prado was supported by grant of Assistant Researcher from the IPANEMA - Industry of Veterinary Products.

References

Abd El-Latif ST, Ahmed KM, Elkalashy SI, Zaki MF (2024) Atmospheric–pressure DBD plasma modifying photoemission, optical and electrical properties of polycarbonate

films. Inorg Chem Commun 161:112048. https://doi.org/10.1016/J.INOCHE.2024.112048

Achee NL, Grieco JP (2018) Current Evidence, New Insights, Challenges and Future Outlooks to the Use of Spatial Repellents for Public Health What Are Spatial Repellents?

Bedrouni F, Ouchabane M, Almabouada F, Saidi-Amroun N (2024) Isotactic-polypropylene (iPP) wettability modified by surface DBD plasma. Phys Scr 99:075919. https://doi.org/10.1088/1402-4896/ad49e8

Carneiro N, Souto AP, Nogueira C, et al (2006) Preparation of cotton materials using corona discharge. Journal of Natural Fibers 2:53–65. https://doi.org/10.1300/J395v02n04_04

Fatahian R, Erfani R (2025) Surface modification of electrospun nanofibers via nonthermal plasma for wound healing: A comprehensive review. Inorg Chem Commun 180:. https://doi.org/10.1016/j.inoche.2025.115119

Francelino IG, Tavares VKF, Leite LDP, et al (2025) Silver nanoparticle incorporation on polyamide 6,6 fabrics by hybrid corona-dielectric barrier discharge for antimicrobial applications. Journal of Nanoparticle Research 27:. https://doi.org/10.1007/s11051-025-06252-y

Gawish SM, Ramadan AM, Cornelius CE, et al (2007) New Functionalities of PA6,6 Fabric Modified by Atmospheric Pressure Plasma and Grafted Glycidyl Methacrylate Derivatives. Textile Research Journal 77:92–104. https://doi.org/10.1177/0040517507076747

Ghosh J, Rupanty NS, Noor T, et al (2025) Functional coatings for textiles: advancements in flame resistance, antimicrobial defense, and self-cleaning performance. RSC Adv. 15:10984–11022

Grinberg Francelino I, de Souza Miranda F, Gasi F, et al (2025) Silica Deposition on Polyamide 6,6 Fabrics by Hybrid Corona-Dielectric Barrier Discharge Plasma. Materials Research 28:. https://doi.org/10.1590/1980-5373-MR-2024-0257

Hossain MdT, Reza S, Islam MdA, et al (2025) Progress and Prospects of Chemical Functionalization of Textiles Via Nanotechnology. ACS Applied Engineering Materials 3:1–20. https://doi.org/10.1021/acsaenm.4c00644

Javadzadeh Y, Hamedeyaz S (2014) Floating Drug Delivery Systems for Eradication of Helicobacter pylori in Treatment of Peptic Ulcer Disease. Trends in Helicobacter pylori Infection. https://doi.org/10.5772/57353

Kuhr M, Synytska A, Bellmann C, et al (2016) Methods for a permanent binding of functionalized micro-particle on polyester fabric for the improvement of the barrier effect. Journal of Industrial Textiles 46:643–663. https://doi.org/10.1177/1528083715584139

Luo S, Van Ooij WJ (2002) Surface modification of textile fibers for improvement of

adhesion to polymeric matrices: A review. J Adhes Sci Technol 16:1715–1735. https://doi.org/10.1163/156856102320396102

Morent R, De Geyter N, Verschuren J, et al (2008) Non-thermal plasma treatment of textiles. Surf Coat Technol 202:3427–3449. https://doi.org/10.1016/j.surfcoat.2007.12.027

Morro A, Catalina F, Pablos JL, et al (2017) Surface modification of poly(ε-caprolactone) by oxygen plasma for antibacterial applications. Biocompatibility and monitoring of live cells. Eur Polym J 94:405–416. https://doi.org/10.1016/j.eurpolymj.2017.07.027

Mou Y, Zuo C, Wu Y, et al (2024) Surface modification of carbon-based materials using a double dielectric barrier discharge for efficient removal of OPFRs with different polarity. Journal of the Indian Chemical Society 101:101112. https://doi.org/10.1016/J.JICS.2023.101112

Muñoz V, Buffa F, Molinari F, et al (2019) Electrospun ethylcellulose-based nanofibrous mats with insect-repellent activity. Mater Lett 253:289–292. https://doi.org/10.1016/j.matlet.2019.06.091

Nadi A, Boukhriss A, Bentis A, et al (2018) Evolution in the surface modification of textiles: a review. Textile Progress 50:67–108. https://doi.org/10.1080/00405167.2018.1533659

Nascimento L, Gasi F, Landers R, et al (2020) Physicochemical studies on the surface of polyamide 6.6 fabrics functionalized by DBD plasmas operated at atmospheric and sub-atmospheric pressures. Polymers (Basel) 12:. https://doi.org/10.3390/POLYM12092128

Ojstršek A, Jug L, Plohl O (2022) A Review of Electro Conductive Textiles Utilizing the Dip-Coating Technique: Their Functionality, Durability and Sustainability. Polymers (Basel). 14

Peran J, Ercegović Ražić S (2020) Application of atmospheric pressure plasma technology for textile surface modification. Textile Research Journal 90:1174–1197

Petraconi A, Miranda F, Prado E, et al (2023) Hybrid Corona–Dielectric Barrier Discharge for Permethrin Polymerisation on Polyamide Fabric at Atmospheric Pressure. Fibers and Polymers 24:373–382. https://doi.org/10.1007/s12221-023-00058-2

Ribeiro AI, Modic M, Cvelbar U, et al (2020) Effect of dispersion solvent on the deposition of PVP-silver nanoparticles onto DBD plasma-treated polyamide 6,6 fabric and its antimicrobial efficiency. Nanomaterials 10:. https://doi.org/10.3390/nano10040607

Ribeiro AI, Senturk D, Silva KS, et al (2018) Efficient silver nanoparticles deposition method on DBD plasma-treated polyamide 6,6 for antimicrobial textiles. In: IOP Conference Series: Materials Science and Engineering. Institute of Physics

Publishing
SHEN 沈 J剑, WANG 王 F法军, WEI 魏 W伟, et al (2025) Surface modification of fabrics using dielectric barrier discharge plasma for improved antifouling performance. Plasma Science and Technology 27:014001. https://doi.org/10.1088/2058-6272/ad8da6
Singh M, Vajpayee M, Ledwani L, et al (2023) Study of physico-chemical and antibacterial properties of DBD plasma treated ahimsa silk coated with natural active agent. Phys Scr 98:065001. https://doi.org/10.1088/1402-4896/accee2
Singh S, Prakash C, Wang H, et al (2019) Plasma treatment of polyether-ether-ketone: A means of obtaining desirable biomedical characteristics. Eur Polym J 118:561–577. https://doi.org/10.1016/j.eurpolymj.2019.06.030
Sukkanon C, Bangs MJ, Nararak J, et al DISCRIMINATING LETHAL CONCENTRATIONS FOR TRANSFLUTHRIN, A VOLATILE PYRETHROID COMPOUND FOR MOSQUITO CONTROL IN THAILAND
Tawiah B, He W, Seidu RK, et al (2025) Mosquito-repellent textiles: a systematic review of material innovations, application principles and research trends. Textile Research Journal
Tsafack MJ, Levalois-Grützmacher J (2006) Plasma-induced graft-polymerization of flame retardant monomers onto PAN fabrics. Surf Coat Technol 200:3503–3510. https://doi.org/10.1016/j.surfcoat.2004.11.030
Vesin A, Glorennec P, Le Bot B, et al (2013) Transfluthrin indoor air concentration and inhalation exposure during application of electric vaporizers. Environ Int 60:1–6. https://doi.org/10.1016/j.envint.2013.07.011
Vu NK, Zille A, Oliveira FR, et al (2013) Effect of particle size on silver nanoparticle deposition onto dielectric barrier discharge (DBD) plasma functionalized polyamide fabric. Plasma Processes and Polymers 10:285–296. https://doi.org/10.1002/ppap.201200089
Wagman JM, Achee NL, Grieco JP (2015) Insensitivity to the Spatial Repellent Action of Transfluthrin in Aedes aegypti: A Heritable Trait Associated with Decreased Insecticide Susceptibility. PLoS Negl Trop Dis 9:. https://doi.org/10.1371/journal.pntd.0003726
Zhongfu R, Xiaoliang T, Hong'en W, Gao Q (2007) Continuous modification treatment of polyester fabric by Ar-O2 (10:1) discharge at atmospheric pressure. Journal of Industrial Textiles 37:43–53. https://doi.org/10.1177/1528083707078082
Zille A, Fernandes MM, Francesko A, et al (2015) Size and Aging Effects on Antimicrobial Efficiency of Silver Nanoparticles Coated on Polyamide Fabrics Activated by Atmospheric DBD Plasma. ACS Appl Mater Interfaces 7:13731–13744. https://doi.org/10.1021/acsami.5b04340